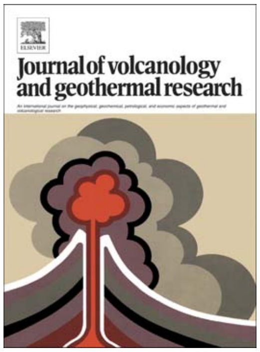

Numerical simulation of plagioclase rim growth during magma ascent at Bezymianny Volcano, Kamchatka

N.V. Gorokhova, O.E. Melnik, P.Yu. Plechov, V.D. Shcherbakov

PII: S0377-0273(13)00096-6
DOI: doi: 10.1016/j.jvolgeores.2013.03.020
Reference: VOLGEO 5114

To appear in: *Journal of Volcanology and Geothermal Research*

Received date: 29 December 2011
Accepted date: 22 March 2013

Please cite this article as: Gorokhova, N.V., Melnik, O.E., Plechov, P.Yu., Shcherbakov, V.D., Numerical simulation of plagioclase rim growth during magma ascent at Bezymianny Volcano, Kamchatka, *Journal of Volcanology and Geothermal Research* (2013), doi: 10.1016/j.jvolgeores.2013.03.020

Numerical simulation of plagioclase rim growth during magma ascent at Bezymianny Volcano, Kamchatka

Gorokhova N.V.[1], Melnik O.E.[1], Plechov P.Yu.[2] , Shcherbakov V.D.[2]

[1]Institute of Mechanics, Moscow State University

[2]Geology Department, Moscow State University

Abstract

Slow CaAl-NaSi interdiffusion in plagioclase crystals preserves chemical zoning of plagioclase in detail, which, along with strong dependence of anorthite content in plagioclase on melt composition, pressure, and temperature, make this mineral an important source of information on magma processes. A numerical model of zoned crystal growth is developed in the paper. The model is based on equations of multicomponent diffusion with diagonal cross-component diffusion terms and accounts for mass conservation on the melt-crystal interface and growth rate controlled by undercooling. The model is applied to the data of plagioclase rim zoning from several recent Bezymianny Volcano (Kamchatka) eruptions. We show that an equilibrium growth model cannot explain crystallization of naturally observed plagioclase during magma ascent. The developed non-equilibrium model reproduced natural plagioclase zoning and allowed magma ascent rates to be constrained. Matching of natural and simulated zoning suggests ascent from 100 to 50 MPa during 15 - 20 days. Magma ascent rate from 50 MPa to the surface varies from eruption to eruption: plagioclase zoning from the December 2006 eruption suggests ascent to the surface in less than 1 day, whereas plagioclase zoning from March 2000 and May 2007 eruptions are better explained by magma ascent over periods of more than 30 days). Based on comparison of diffusion coefficients for individual elements a mechanism of atomic diffusion during plagioclase crystallization is proposed.

1. Introduction

Decompression-driven crystallization is a widespread phenomenon in water-rich silicic magmas (e.g. Cashman, 1992; Blundy and Cashman, 2001; Hammer and Rutherford, 2002; Blundy et al., 2006; Brugger and Hammer, 2010). It occurs during final magma ascent from the magma storage region to the surface prior eruption when water content in magma exceeds water solubility. Rapid crystallization induced by fast magma ascent may lead to formation of a boundary layer on the crystal-melt boundary depleted in components of growing mineral due to relatively slow diffusion in silicic melts. In that case growing mineral would not be in equilibrium with the main volume of the melt and only local equilibrium between boundary layer and a crystal would be attained. Such crystallization is referred as non-equilibrium. Experimental studies of decompression-driven crystallization (e.g. Geschwind and Rutherford, 1995; Martel and Schmidt, 2003; Brugger and Hammer, 2010; Mollard et al., 2012) show that decompression rate strongly affects morphology and composition of plagioclase, which become enriched in albite with an increase of decompression rate. That relation makes possible to interpret morphology and composition of groundmass minerals of volcanic rocks and estimate rates of magma ascent.

There were numerous studies which simulated plagioclase grow and interpreted formation of complex compositional zoning. Allegre et al. (1981), Lasaga (1982), L’Heureux (1993), L’Heureux and Fowler (1996), and Tsune and Toramaru (2007) proposed different explanations for the zoning in plagioclase crystals. In all of these studies the crystal growth process was described by a one-dimensional (1D) diffusion equation (or system of equations for a multicomponent mixture) in the coordinate system moving with the crystal surface.

Allegre et al. (1981) suggested that the crystal zoning develops as the result of a special dependence of the growth rate on the Ab concentration in the melt boundary layer in the form of a three-valued function, which makes transitions from one regime of crystal growth to the other possible. However, this growth law was not confirmed experimentally. Experiments by Kirkpatrick et al. (1979), Hammer and Rutherford (2002), Couch et al. (2003), and in several other studies suggest that crystal growth rate is a bell-shaped function of the temperature or undercooling that can be expressed as a function of melt composition.

Lasaga (1982) proposed formulas based on experimental data for calculating the liquidus temperature and the crystal growth rate which depend on the melt undercooling in the boundary layer. It was postulated that if different values (up to three) of the crystal growth rate are possible for the same melt composition, transitions between the regimes of rapid and slow crystal growth result in the appearance of zoning in the crystal.

L'Heureux and Fowler (1996) used the crystal growth model of Lasaga (1982). Stability of the solution of the diffusion equation linearized in the neighbourhood of the stationary solution was investigated. These authors found ranges of the partition coefficient K (the crystal-to-melt-component concentration ratio) that lead to instability. According to this study zoning forms only when $K<1$. L'Heureux (1993) proposed a more complicated formula for calculating crystal growth rate which reflects the dependence of growth rate on crystal surface nucleation and thermodynamic characteristics. Their linear stability analysis also showed that crystal zoning may appear only if $K<1$. L'Heureux and Fowler (1996) and L'Heureux (1993) used isothermal models and two-component systems, which were described by a single diffusion equation. Likewise L'Heureux (1993) assumed a simple linear relationship between the component concentrations in the crystal and in the melt. However, the inequality $K<1$ is not typical of plagioclase crystal growth from water-saturated magmas in natural conditions (Housh and Luhr, 1991)

Tsune and Toramaru (2007) proposed a formula for calculating growth rate as a function of crystal roughness. As a crystal grows, the face is filled and the growth rate changes stepwise from the regime corresponding to a rough wall to a slower regime corresponding to a smooth wall. Then, in the smooth growth regime, due to melt enrichment the growth rate begins to increase and changes back to the rough growth regime in a stepwise manner. The model explains oscillations of crystal composition but the oscillation period is determined by the position of the transitions between the regimes.

Oishi (1965) investigated a 1D system of equations describing diffusion in a three-component system analytically and numerically accounting for cross terms in the expressions for mass fluxes resulted in nonlinearity of the system. The system solutions were analyzed depending on the relationships between the component diffusion coefficients.

Gorokhova and Melnik (2010) considered the process of diffusion growth of a single crystal from cooling melt. To capture the complexity of the natural process, the nonlinear system of diffusion equations proposed by Oishi (1965) was used to describe the diffusion crystal growth. The cooling of the melt and the dependence of component diffusion coefficients on melt temperature were taken into account. It was shown that zoning may arise as a result of melt cooling (even if the temperature decreases linearly) for the case when crystal growth rate can be uniquely determined from melt temperature and composition.

The model of Gorokhova and Melnik (2010) simplifies the magmatic melt to three components: An, Ab, and residual melt. The first two components form plagioclase crystals. Melt composition changes during crystal growth. This model does not account for the complexity of the real magmatic melt composition and diffusing species. Although there are experimental data for different natural and synthetic compositions at a wide range of pressure and temperature (Chakraborty et al., 1995a, Chakraborty et al., 1995b, Liang et al., 1996, Zhang et al., 2010), it is not possible to reconstruct a complete diffusion matrix for a range of compositions at Bezymianny Volcano.

This study expands the model of Gorokhova and Melnik (2010) by considering a decompression-induced crystallization, during which the dependence of crystal composition and the liquidus temperature on pressure and melt composition are taken into account. Our basic concept of rim formation is applied to plagioclase crystals from lavas of Bezymianny volcano investigated by Shcherbakov et al. (2011). There are many speculations that plagioclase rims similar to those in samples from Bezymianny may form due to injections of mafic magma (e.g. Murphy et al., 2000), self-convection in magma chamber (e.g. Couch et al., 2001, Rutherford and Devine, 2008) or magma decompression during ascent (e.g. Blundy et al., 2006). Since modelled rims zoning of phenocrysts is similar to zoning of microphenocrysts and microlites we argue that rims form mainly in response to decompression in volcanic conduit, while magma injection and convection may influence initial conditions of the ascent such as magma temperature and composition.

Calculated compositional profiles were compared with measured electron microprobe traverses across plagioclase crystals from different eruptions of Bezymianny volcano (2000, 2006 and 2007 eruptions were chosen for comparison, Fig. 1) in order to constrain the timescales of magma ascent.

FIG 1

2. Formulation of the problem

We will consider the crystallization process in a 1D system consisting of a crystal and melt separated by a moving interface, the crystallization front. We introduce the coordinate system where the crystal growth starts as the plane ($x = 0$, Fig. 2). On the moving interface ($x = s$) between the melt and the crystal the mass conservation laws for An and Ab are satisfied. On the outer domain boundary ($x = L$) no mass flux condition is postulated. This assumption is valid if on the right there is another cell with a growing crystal, so that at the interface between the cells the mass flux vanishes. Of course, this system geometry does not reflect the complexity of the phenomenon in full detail, but makes it possible to investigate the main features of the crystal growth. The cell size is determined by the mean distance between phenocrysts in recent eruptive products of Bezymianny volcano.

FIG 2

The growth of a plagioclase crystal consisting of only two components, An and Ab, is considered. Therefore, we assume that the melt consists of three components: An, Ab, and the residual melt, all with the same densities. This system is oversimplified in comparison to the natural magmatic melt but currently there is a lack of experimental data on inter-diffusivities of melt oxide components in natural water-saturated systems. Thus we tuned diffusion coefficients of the components in order to fit observations of natural samples from Bezymianny Volcano.

Real dependences of the liquidus temperature and crystal composition on melt composition and pressure are used. These dependences are obtained by interpolating data which was calculated with the PETROLOG3 algorithm (Danyushevsky and Plechov, 2011) and are described in the next section.

2.1 Estimation of liquidus temperature and crystal composition.

Liquidus temperature of plagioclase was described as a function of melt composition, pressure, and water content. Plagioclase composition in equilibrium with melt could be defined by the same parameters plus equilibrium temperature. The simulation of non-equilibrium crystallization required the additional assumption that local equilibrium exists during crystallization. In other words, liquidus temperature and plagioclase composition could be defined to be in equilibrium with melt, which is next to the growing crystal interface.

Bulk melt composition was estimated from glassy melt inclusions in orthopyroxene phenocrysts from a 2006 Bezymianny eruption (Shcherbakov et al., 2011). Compositions of melt inclusions suggest that there was no post-entrapment crystallization of host mineral (see Appendix 1), and thus they may be used an approximation of melt composition. We calculated an average melt inclusion composition and decomposed it into 3 components: albite (Ab), anorthite (An), and residual melt (which does not contain a plagioclase component). Then, we calculated a 5% three dimensional (3D) grid with different proportions of residual melt, Ab, and An. At each point on the 3D grid the water saturation was assumed (according to the model of Moore et al. (1998)) to lie in a 0.1 to 200 MPa range of pressure. Crystallization temperatures and plagioclase compositions were determined for water-saturated conditions with a plagioclase-melt equilibrium model (Pletchov and Gerya, 1998) for each point on the 3D grid of hypothetical melts. We chose this plagioclase-melt model because among all known models only the Pletchov and Gerya (1998) model could estimate crystallization temperature with taking into account the influence of water activity in melt on plagioclase composition on the basis of simple plagioclase-melt exchange reaction; this influence may be the main factor controlling plagioclase zoning in water-rich magmas (Housh and Luhr, 1991; Putirka, 2005; Lange et al., 2009). All calculations outlined above were performed using PETROLOG-3 algorithm (Danyushevsky and Plechov, 2011).

3. Equilibrium crystal growth.

The first set of simulations was performed for equilibrium plagioclase growth. In this approach component diffusion is infinitely fast so melt composition across the whole simulation domain remains constant and is determined by equilibrium with the growing crystal. This model can be described by the following system of equations:

$$C_{1S} = C_S(p, C_1, C_2) \tag{1}$$

$$T_{liq} = T_l(p, C_1, C_2) \tag{2}$$

$$f(\xi) = C_{1S}\big|_{\xi} \tag{3}$$

$$M_{1S}(\xi) = \int_0^{\xi} f(x)dx \tag{4}$$

$$M_{1S}(\xi) + C_1(1-\xi) = C_1^0 \tag{5}$$

$$M_{2S}(\xi) + C_2(1-\xi) = C_2^0 \Leftrightarrow (\xi - M_{1S}(\xi)) + C_2(1-\xi) = C_2^0 \tag{6}$$

Here subscripts 1 and 2 correspond to An and Ab, respectively; C_{1S} is the An concentration in a crystal; $M_{iS}(\xi)$ are the total dimensionless masses of components *i* =1,2 inside the crystal; C_i is the concentration of component *i* in the melt; C_i^0 is the total/initial concentration of component *i* in the system; $\xi = \frac{s}{L}$ is the dimensionless position of a crystal-melt boundary (s is the dimensional location of a crystal-melt boundary and *L* is the size of the cell that contains a growing crystal and a surrounding melt); and *f*(*x*) represents the distribution of An inside the crystal (see Fig. 2). Because density variation during crystal growth is neglected *L* remains constant. We assume that only melt inside the cell feeds the growing crystal.

Equations (1-2) describe the dependence of crystal composition and liquidus temperature on melt composition and pressure calculated by Petrolog3 software, (3) is an assumption of local equilibrium, (4) is the definition of the component masses in the crystal, and (5-6) describe mass conservation for An and

Ab components in the system, respectively. Initial melt composition (C_1^0, C_2^0) fits the criteria of equilibrium with the crystal at $\xi = 0$ and the given temperature and pressure.

At equilibrium the temperature of the system is equal to the liquidus temperature. In order to check the consistency of the model the system temperature was calculated independently, assuming the release of latent heat of crystallization:

$$T_{sys} = T_0 + \frac{L_h}{c_V}\xi \tag{7}$$

where $L_h = 3.5 \cdot 10^5\, J/kg$ is latent heat of crystallization, and $c_V = 1200\, J/(kg \cdot K)$ is specific heat capacity. The model gives consistent results if $T_{sys} = T_{liq}$ during the whole crystallization process. As will be shown below, the data from plagioclase rim growth cannot be explained by the equilibrium model.

C_1 and C_2 can be found as a function of ξ from equations (3-6) and then substituted into equations (1,2) leading to equation system (8):

$$\begin{cases} C_{1S} = C_S(p, C_1(\xi), C_2(\xi), \xi) = f_1(p, \xi) \\ T_{liq} = T_l(p, C_1(\xi), C_2(\xi), \xi) = f_2(p, \xi) \end{cases} \tag{8}$$

To solve this equation system An content of the crystal as a function of ξ is required. We approximated An content in the plagioclase rims of several natural compositional profiles with an approximation function (9) (Fig. 3, solid line):

$$f(s) = 0.74 - 4.55s - 416s^2 + 2.2 \cdot 10^4 s^3 - 2.9 \cdot 10^5 s^4 \tag{9}$$

The pressure then can be found from equation (1), while liquidus temperature can be found after substituting the pressure from equation (1) into equation (2).

Solution of the equation system allows pressure, melt composition, and liquidus temperature to be calculated as a function of ξ. Calculated pressure initially decreases and then increases up to 200 MPa (Fig. 3, dashed line)

FIG 3

Since rim growth occurs during magma ascent the pressure increase is impossible; thus, we considered the possibility that pressure stays constant as it reaches its minimum, and subsequent crystal growth is driven by cooling. System (1-6) for a fixed pressure allows temperature to be calculated. Alternatively, a combination of pressure drop and cooling can be proposed.

Calculations were carried out at initial pressures of 100±10 MPa and temperatures of 860±10°C. The starting melt composition provides a constant crystal composition at $s(\xi) = 0$ for given temperatures and pressures; thus, the starting melt composition varies between runs. Results of the calculations are shown in Fig. 4.

FIG 4

Equilibrium approach leads to two stages of crystal growth. At first the crystal grows due to the pressure drop as the magma ascends, then, solution of equations (8) leads to pressure increase (which is unlikely in natural system) and subsequent growth must involve magma cooling. Simulation results strongly depend on the initial pressure and especially on the temperature. The estimated temperature change cannot be explained by release of latent heat of crystallization because in most cases the increase of liquidus temperature exceeds the changes in system temperature. There are several possible explanations for this inconsistency of results. First, there can be simultaneous crystallization of other minerals leading to additional latent heat release. Petrological analysis of samples from Bezymianny eruptions shows that this may have a minor effect that can contribute 5-10% of the temperature rise. Second, samples were possibly taken from the marginal zone of the conduit where shear heating leads to increased temperature. Costa et al. (2007) show that the thickness of this marginal zone can be on the order of one meter; thus, the amount of magma that experiences shear heating is relatively small. The possibility that all three samples from different eruptions experienced shear heating is negligible. Below we show that the non-equilibrium model allows us to explain carefully measured compositional profiles and to place constraints on the magma ascent time.

4. Non-equilibrium crystal growth: mathematical model

We assume that the initial distribution of each melt component's concentrations is determined by that component's total content in the system and remains constant across the simulation domain:

$$C_i(x, t=0) = C_i^0 = const\,,\ i = 1, 2, 3 \tag{10}$$

Here, C_i is the concentration of the melt *i*-component (i = 1: An, 2: Ab, 3: residual melt). The crystal grows when the melt temperature is below the liquidus temperature. For a fixed starting melt composition the liquidus temperature increases with pressure decrease due to water saturation of the melt (see Appendix 1). Thus, magma ascent leads to an effective undercooling and consequent crystal growth. The mathematical model and results of simulations are presented below.

4.1 Equations and boundary conditions

We considered diffusion-controlled growth of plagioclase crystals. The following system of equations (Oishi, 1965) describes 1D multicomponent diffusion in the melt:

$$\begin{aligned}
&\frac{\partial C_i}{\partial t} = -\frac{\partial J_i}{\partial x} \quad , \quad i = 1,\ 2,\ 3 \\
&J_i = -D_i \frac{\partial C_i}{\partial x} - C_i \sum_{i \neq j} (D_i - D_j) \frac{\partial C_j}{\partial x} \\
&\sum_i C_i = 1 \\
&s < x < L, \quad t > 0
\end{aligned} \tag{11}$$

Here, D_i are the diffusion coefficients in the melt phase $s < x < L$ and J_i are the *i*-component mass fluxes. The model takes into account the cross-component diffusion (the second term in the flux formulas) that develops if the component diffusion coefficients are different.

This system of equations was solved only in the melt domain ($s < x < L$) with a moving boundary. Diffusion in the crystal is neglected since it is several orders of magnitude slower than in the melt (Costa et al., 2008). The An and Ab diffusion coefficients are assumed constant. We introduced the relative diffusion coefficient as $C_D = D_2 / D_1$. The residual-melt diffusion coefficient was assumed to be small in comparison with the An and Ab diffusion coefficients, and also constant. Heat diffusion was neglected since the thermal diffusivity is several orders of magnitude higher than the component diffusion. Therefore, within the cell the temperature equalization can be assumed to be instantaneous.

The initial conditions are specified by Eq. (10). On the moving crystal surface $x = s$ is the boundary condition – mass conservation for all components is described by $V[C_i] - [J_i] = 0$. Moving at velocity V from the melt to the boundary, the *i*-component mass flux is $V C_i\big|_0 - J_i\big|_0$ and the mass flux into the crystal is $V\,C_i|_S$. Here $[C_i]$ and $[J_i]$ are the *i*-component concentration and flux jumps on the melt-crystal interface, respectively. Diffusive flux within the crystal is negligibly small. At $x = L$ the mass fluxes J_i vanish. Thus, for system (11) the boundary conditions are

$$\begin{aligned} x = s: &\quad V(\Delta T)(C_i|_{x=s} - C_{i;S}) - J_i|_{x=s} = 0 \\ x = L: &\quad \left.\frac{\partial C_i}{\partial x}\right|_{x=L} = 0, \qquad i = 1,2,3 \end{aligned} \tag{12}$$

Here $C_{i;S}$ is the *i*-component concentration in the crystal (the crystal consists of components 1 and 2 only; $C_{3;S} = 0$). $V(\Delta T)$ is the linear crystal growth rate that depends on effective undercooling $\Delta T = T - T_{liq}$.

4.2 The growth rate

The crystal growth rate $V(\Delta T)$ is described by a bell-shaped function (Hort, 1998; Melnik and Sparks, 2005):

$$V = V_0 \frac{-\Delta T \cdot T_u}{(T - \Delta T - T_u)T} \cdot \exp\left(-\frac{(T_u - T)(T - \Delta T)}{(T - \Delta T - T_u)T} \right) \tag{13}$$

Here, T_u is the temperature at which the growth rate reaches the maximum, V_0. Undercooling corresponding to maximum growth is assumed constant and equal to 62 ^{0}C. Equation (13) was successfully applied for modelling crystal growth during lava-dome-building eruptions on the Soufriere Hills Volcano, Montserrat (Melnik and Sparks, 2005), Shiveluch Volcano, Russia (Dirksen et al., 2006), and Mount St Helens, USA (Melnik et al., 2011). We assume that the melt temperature T increases as a consequence of latent heat release.

Domain size, $L = 0.35\ mm$, is the same as for the equilibrium calculations. We used the following initial conditions which fit a criteria of chemical equilibrium of the starting melt and a crystal: $An_{S0} = 0.74$, $T_{liq0} = 850°C$, $p_0 = 100\ MPa$. The temperature is equal to the plagioclase liquidus temperature at $t = 0$ and changes with time following (7). If external cooling is taken into account this equation becomes $T_{sys} = T_0 - \max\left(0, V_T(t - t_0)\right) + \frac{L_h}{c_V} \times \frac{s}{L}$ where V_T is the cooling rate and t_0 is the moment when cooling starts.

We have tested different system evolution scenarios in order to determine governing parameters and estimate uncertainties. The pressure drop during magma ascent is controlled by the gravity force, conduit resistance, conduit cross-section area, and discharge rate. For steady state ascent conditions it can be estimated from the solution of the following equation:

$$\frac{d}{dx} p = -\rho g - \lambda \frac{\rho V^2}{2d} . \tag{14}$$

Here x is a vertical coordinate, ρ is the density of magma, g is the gravity acceleration, λ is the conduit friction coefficient, V is ascent velocity, and d is the conduit diameter. For the laminar flow $\lambda = 64/\mathrm{Re}$ where $\mathrm{Re} = \rho V d/\mu$ is the Reynolds number, μ is the magma viscosity. If all coefficients on the right hand side of (14) are constant the pressure drops linearly with height and an ascending parcel of magma experiences a linear decrease in pressure with time. Due to rheological stiffening in the upper part of the conduit, pressure gradients can increase dramatically (Melnik and Sparks, 1999). If an explosive event occurs a parcel of magma can be rapidly propelled from high to atmospheric pressure; subsequently rapid cooling in a volcanic column or slow cooling in a pyroclastic flow can occur.

5. Results

For the first set of simulations we assume that pressure drops from an initial value down to atmospheric over 15 days at a steady rate. Because diffusion coefficients for An and Ab cannot be directly measured in experiments, we explored wide ranges of diffusion coefficients assuming that they were constant. Their ratios varied as $C_D = 0.1,\ 0.3,\ 1,\ 10$ ($C_D = \frac{D_{Ab}}{D_{An}}$) with a characteristic value of $D_1 = 1,\ 10,\ 100\, x 10^{-14}\ m^2/s$ ($D_1 = D_{An}$). Diffusion coefficients depend on the temperature and water content of the magma through the Arrhenius relationship $D = D_0 e^{-\frac{E}{kT}}$. These parameters have an opposite effect on the diffusion rate during magma ascent: temperature increase due to latent heat release intensifies diffusion, whereas water exsolution in response to pressure decrease leads to slower diffusion. As a first order of approximation we assume that the diffusion coefficient is constant.

Figure 5(a) shows calculated and measured compositional profiles within the crystal for different ratios of diffusion coefficients C_D and values of D_1, and 5(b) illustrates crystal size as a function of time.

FIG 5

Crystals of smaller size form at lower diffusion rates because the boundary layer becomes depleted in plagioclase components and the growth stops. An content along core-to-rim profiles of small crystals decreases much faster than measured data. Crystal size strongly depends on C_D; smaller C_D leads to formation of smaller crystals.

Simulations with different maximum linear growth rate values V_0 indicate that this parameter does not significantly influence crystal growth. A relatively large influence was observed only at low values of V_0, because at a low rate the degree of non-equilibrium increases even at high diffusion rates since the crystal cannot efficiently grow in response to undercooling (Fig 6a and 6b).

FIG 6

Figure 7a and 7b show simulation results under different conditions of magma ascent. Different lines correspond to stepwise changes in ascent rate of a magma parcel that can occur due to increase/decrease of discharge rate or changes of pressure gradient as the magma parcel ascends. A decrease in the rate of pressure drop results in a slower decrease of An content and in some cases even in an increase of An as the crystal grows. Faster diffusion reduces the influence of the ascent rate, because crystallization drives the system faster towards equilibrium.

FIG 7

The best fit for the first stage of crystal growth (s $\le$ 0.02 mm) corresponds to $D_1 = 10^{-13}\ m^2/s$ and $C_D = D_2/D_1 = 0.3$ for a magma ascent time between 15 and 20 days (Fig. 8). This timescale is in good agreement with magma ascent timescales for typical lava dome building eruptions. With extrusion rates on the order of 1m^3/s and a conduit diameter of 20-40 m magma ascent time from 3 km depth is between 11 and 43 days.

FIG 8

The ascent time, of course, is defined by particular values of maximum growth rate V_0 and diffusion coefficient D_1. By using the π theorem one can show that the ascent time t_A is a function of the ratio between growth timescale t_V and diffusive timescale t_D:

$$t_A = t_D \pi\left(\frac{t_V}{t_D}\right), t_D = \frac{D_1}{L^2}, t_V = \frac{V_0}{L}.$$

Thus, the same profile inside the crystal can be obtained if diffusion coefficients and growth rate are n times faster for n times shorter ascent time. Several experimental studies of non-equilibrium decompression-induced crystallization in water-saturated silicic magmas provide good constraints on the maximum growth rate. Hammer and Rutherford (2002) explored crystallization of Pinatubo magma under rapid decompression at 780 ^{o}C. In the experiments of Couch et al. (2003) an initial melt composition was estimated for the Soufrière Hills Volcano, Montserrat at 875 ^{o}C. Maximum growth rates resulting from the Hammer and Rutherford (2002) experiments are on the order of 10^{-9} m/s; Couch et al. (2003) obtained similar values at higher temperatures. Brugger and Hammer (2010) studied decompression-induced crystallization of lightly-crushed pyroclasts from the 3430 yr. BP caldera-forming ignimbrite of Aniakchak Volcano in the Aleutian Arc at a rate between 0.5 and 10 MPa/h. They show that typical growth rates are close to 10^{-9} m/s, reaching higher values only for decompression rates of 10 MPa/h, which is not typical for magma ascent conditions during extrusive eruptions. Importantly, the maximum observed growth rates varied little, being almost independent of melt compositions (within a range of high silica magmas) and experimental conditions such as temperature and decompression scenarios.

In order to explain the possible diffusion scenario during plagioclase crystallization we used the data from Zhang et al. (2010) for silicic melts at 850 ^{0}C describing atomic diffusion of individual elements. We consider the diffusion of all major elements listed in Table A-1, namely Na, K, Ca, Mg, Fe, Al, Si, and O. The diffusion of other elements is neglected as their concentrations are either negligible or do not affect the growth of plagioclase. The fastest diffusion rates are documented for Na (~1-3 x 10^{-10} m^2/s for wet rhyolite at 3.5 wt% H_2O) and K (~5x10^{-12} m^2/s at 5.5 wt% H_2O). Mg diffusion is an order of magnitude slower. For dry andesite it is of order of 1.2x10^{-13} m^2/s but according to Mungall et al. (1999) addition of 3.6 wt% H_2O leads to 4ln units increase in diffusion coefficient resulting in D_{Mg} ~ 7x10^{-13} m^2/s). According to Koepke and Behrens (2001), Fe in water-saturated magmas shows a similar value (~1.7x10^{-13} m^2/s). Ca exhibits slower diffusion (~1-3x10^{-14} m^2/s) in dry rhyolite; however, adding H_2O enhances Ca diffusivity significantly. Diffusion coefficients of Si and O are of the same order of magnitude. The ratio of D_{Ca}/D_{Si} is ~ 1-20 according to Watkins et al. (2011), with lower values more common for natural melts. As mentioned by Zhang et al. (2010) "Despite the numerous papers on Al diffusivities, most Al diffusivity data were obtained as side-products. Except for Liang et al. (1996) who investigated Al self-diffusion in a ternary system at a single temperature (1773 K), other studies are all on SEBD of Al in various melts. No tracer diffusivities or FEBD on Al are available. Furthermore, Al diffusion data in some papers are scattered. Hence, Al diffusion in natural silicate melts is not very well constrained". Reported data for dry andesite (equation (35) from Zhang et al., 2010) at 850 ^{0}C gives a value of diffusion coefficient of order of 2x10^{-16} m^2/s but no water saturated data is presented in the literature.

During plagioclase growth Ca diffuses into the growing crystal, while Al and a fraction of SiO_2 is incorporated into the plagioclase. Because residual melt becomes more silica reach some SiO_2 diffuses out of the growing crystal interface. We propose that Al diffusion is negligibly small in comparison with that of other elements on the timescale of crystallization processes, and therefore a growing crystal incorporates Al as the crystal grows. Redistribution of Al occurs due to diffusion of other elements (cross-terms in diffusion equations (11)). Diffusions of Na and K are extremely fast so their concentrations change according to the equilibrium condition. The rate-limited factor is the diffusion of Ca, Mg, Fe, Si, and O, which are within an order of magnitude of each other.

In order to explain the observed An profile for the May 2007 eruption the pressure drop rate must become slower during the second stage of crystallization. The best fit for the data is found when the pressure drop rate decreases by a factor of 2 or more. There is a minor difference between the case of ascent for 30 and for 100 days, suggesting that crystallization occurs very close to equilibrium.

The sample from December 2006 shows a rapid drop in An content after the initial stage of crystallization. As shown in Fig. 8, this can be achieved by rapid (less than 1 day) magma ascent and associated pressure decrease from 48 MPa to atmospheric, or the combination of a relatively slow ascent with rapid cooling. The second scenario seems to be less realistic.

6. Conclusions

In this paper and in Gorokhova and Melnik (2010) we have developed a mathematical model of plagioclase crystal growth based on multicomponent diffusion equations using relations between crystal and melt composition, pressure, and temperature. Simulations were performed using equilibrium assumptions resulted in extremely large calculated temperatures at the end of the rim growth process that cannot be explained by latent heat release and thus seems unlikely. In a non-equilibrium model the temperature of the system is not defined by its equilibrium value; thus, it can change independently. The model allows to constraint magma ascent rates from variation of the plagioclase rim composition.

We fitted phenocryst compositional profiles for three typical eruptions of Bezymianny Volcano by means of simulations based on a non-equilibrium model. The best-fit scenario results in two distinct stages. Initial crystallization during all three eruptions occurs during ascent from 100 to 48 MPa over 15-20 days. Similarity of composition profiles at this stage suggests similarity in ascent conditions. The magma ascent rate during the 2007 eruption must decrease by at least a factor of 2 after the initial stage. Crystal growth approaches equilibrium and it is very difficult to impose accurate constraints on ascent rate for the second stage. To explain the 2006 eruption profiles either 5 K/h cooling or fast ascent (within 1 day) during the second stage of crystallization is required. The second scenario seems to be more realistic. Compositional profiles for the 2000 eruption cannot be reproduced by our model; this may be evidence of other processes besides pressure drop and cooling, for example, crystallization of other minerals.

This study can be used together with other methods and measurements, including ground deformation, dome volume, seismicity, and gas geochemistry to constrain an integrated model of a lava dome building eruption on Bezymianny and similar volcanoes. Only a model that fits multiparametric observations widely available for several volcanoes can have predictive power and more reliably describe eruption evolution.

Acknowledgments. We acknowledge the support from the Russian Foundation for Basic Research (grants 12-05-00941 and 12-01-92601). Reviews by Ralf Dohmen and Ilya Bindeman leaded to major improvement of the manuscript. Comments from Pavel Izbekov and Jon Blundy were very helpful.

APPENDIX 1

The model melt composition was estimated based on composition of glassy melt inclusions in orthopyroxene phenocrysts from the 2006 Bezymyanny eruption. We have analyzed two sets of melt inclusions both in orthopyroxene and in plagioclase phenocrysts. Inclusions composition for both host minerals overlaps each other for most of components, except CaO and Al_2O_3. We suppose that it can be explained by wall crystallization of ~10% of plagioclase. Absence of Mg and Fe depletion of opx-hosted melt inclusions suggest no post-entrapment crystallization of the latter. The average composition of 11 melt inclusions is presented in Table A-1. This composition was normalized to 100% (water-free) and CIPW norms were calculated . Melt composition was divided into 3 major components (Ab: 36.05 wt/%, An: 2.6 wt %, and residual melt: 61.35 wt%) for easy representation in the numeric model. The sum of these major components corresponds to averaged melt inclusions. In modelling procedures we used melt compositions which consisted of residual melt and variable amounts of Ab and An.

Crystal composition and liquidus temperature were plotted versus An content in melt at various pressures, calculated using the equilibrium model. Pressure varies in the range of 0.1-100 MPa. Plotted values of Ab concentration in melt correspond to marginal Ab concentrations at the crystal-melt boundary during crystal growth.

Table A-1. Average melt inclusion (MI) composition used in calculations and its decomposition to Ab, An, and residual melt components. Normative phase proportions are calculated for an average MI composition using the CIPW scheme

Components	**wt. %**	**SiO_2**	**TiO_2**	**Al_2O_3**	**Fe_2O_3**	**FeO**	**MnO**	**MgO**	**CaO**	**Na_2O**	**K_2O**
Ab	36.05	68.74		19.44						11.82	
An	2.60	43.19		36.65					20.16		
Residual melt	61.35	80.42	0.68	6.83	1.24	2.62	0.10	0.85	0.95	0.00	6.31
MI average	**100**	**75.24**	**0.42**	**12.15**	**0.76**	**1.61**	**0.06**	**0.52**	**1.11**	**4.26**	**3.87**

Normative CIPW phase proportions

Qtz	An	Di	Hyp	Ab	Ort	Ilm	Mt
32.34	2.60	2.43	1.83	36.05	22.87	0.80	1.10

FIG A1

Figure captions

Fig.1. Typical plagioclases from Bezymianny Volcano; a: 14 March 2000, b: 24 December 2006, c: 12 May 2007. Anorthite content across the crystals is shown on the plots from rim to core. For more details see Shcherbakov et al. (2011).

Fig.2 Schematic view of the system; I: crystal, II: melt. V is velocity of the crystal-melt interface, J is flux due to component diffusion, L is total cell length, and s is position of the crystal-melt interface. The concentration of An changes within the crystal. The total mass of An (M_{1S}) can be obtained by integrating the An profile along the crystal.

Fig.3. Pressure variation during crystal growth (dashed line) obtained from the equilibrium model (1-6). An content for three eruptions of Bezymianny Volcano (symbols) is approximated by the solid line.

Fig.4. Temperature variation during crystal growth for different initial conditions; a: different initial pressures, b: different initial temperatures. Both liquidus and system temperature increases due to latent heat of crystallization release are shown. The model gives consistent results if liquidus temperature is equal to system temperature. Variations of starting parameters do not lead to consistent results for the equilibrium model.

Fig.5 Influence of $C_D = D_2/D_1$ and D_1 on the An profile in crystal (a) and on crystal size (b) in the case of the non-equilibrium model.

Fig.6. Influence of maximum growth rate on plagioclase composition (a) and size of the growing crystal (b).

Fig. 7. Influence of different ascent scenarios and diffusion rates on the plagioclase composition (a) and size of the growing crystal (b).

Fig.8. Fitting the model parameters for compositional profiles of particular eruptions.

Fig.A1. Dependence of crystal An content and liquidus temperature on the melt phase AN content at different pressures.

References

Allegre, C.J., Provost, A., Jaupart, C., 1981. Oscillatory Zoning: a Pathological Case of Crystal Growth. Nature 294, 223–228.

Blundy, J., Cashman, K.V, 2001. Ascent-driven crystallisation of dacite magmas at Mount St Helens, 1980-1986. Contrib. Mineral. Petr. 140, 631-650.

Blundy, J., Cashman, K.V., Humphreys, M.C.S., 2006. Magma heating by decompression-driven crystallization beneath andesite volcanoes. Nat. 443, 76-80.

Brugger, C.R., Hammer, J.E., 2010. Crystallization kinetics in continuous decompression experiments; implications for interpreting natural magma ascent processes. J. Petrology, 51, 1941-1965.

Cashman, K.V., 1992. Groundmass crystallization of Mount St. Helens dacite, 1980-1986: A tool for interpreting shallow magmatic processes. Contrib. Mineral. Petrol. 109, 431-449.

Chakraborty, S., Dingwell, D.B., Rubie, D.C., 1995a. Multicomponent diffusion in ternary silicate melts in the system K_20-$A1_20_3$-$Si0_2$: I. Experimental measurements. Geochimica et Cosmochimica Acta 59 (2), 255-264.

Chakraborty, S., Dingwell, D.B., Rubie, D.C., 1995b. Multicomponent diffusion in ternary silicate melts in the system K_20-$A1_20_3$-$Si0_2$: II. Mechanisms, systematics, and geological applications. Geochimica et Cosmochimica Acta 59 (2), 265-177.

Costa, A., Melnik, O., Vedeneeva, E., 2007. Thermal effects during magma ascent in conduits. J. Geophys. Res. 112, B12205, doi: 10.1029/2007JB004985.

Costa, F., Dohmen, R., Chakraborty S., 2008. Time scales of magmatic processes from modeling the zoning patterns of crystals. Reviews in Mineralogy and Geochemistry 69 , 545-594.

Couch, S., Sparks, R. S. J. & Carroll, M. R. (2001). Mineral disequilibrium in lavas explained by convective self-mixing in open magma chambers. Nature 411, 1037–1039.

Couch, S., Harford, C.L., Sparks, R.S.J., Carroll, M.R., 2003. Experimental constraints on the conditions of formation of highly calcic plagioclase microlites at the Soufrière Hills Volcano, Montserrat. J. Petrol. 44, 1455-1475.

Danyushevsky, L.V., Plechov, P., 2011. Petrolog3: Integrated software for modelling crystallization processes. Geochem. Geophys. Geosyst. 12, Q07021, doi:10.1029/2011GC003516.

Dirksen, O., Humphreys, M.C.S., Plechov, P., Melnik, O., Demyanchuk, Y., Sparks, R.S.J., Mahony, S., 2006. The 2001–2004 dome-forming eruption of Shiveluch Volcano, Kamchatka: observation, petrological investigation and numerical modelling. Journal of Volcanology and Geothermal Research, doi:10.1016/j.jvolgeores.2006.03.029.

Geschwind, C.H., Rutherford, M.J., 1995. Crystallization of microlites during magma ascent: the fluid mechanics of 1980-1986 eruption at Mount St Helens. Bull Volcanol, 57, 356-370.

Gorokhova, N.V., Melnik, O.E., 2010. Modelling of the Dynamics of Diffusion Crystal Growth from a Cooling Magmatic Melt. Fluid Dynamics 45 (5), 679-690, DOI: 10.1134/S0015462810050017.

Hammer, J.E., Rutherford, M.J., 2002. An experimental study of the kinetics of decompression-induced crystallization in silicic melt. J Geophys Res 107 (B1), doi:10.1029/2001JB000281.

Hort, M., 1998. Abrupt Change in Magma Liquidus Temperature Because of Volatile Loss or Magma Mixing: Effects of Nucleation, Crystal Growth and Thermal History of the Magma. J. Petrology 39 (5), 1063–1076.

Housh, T.B., Luhr, J.F., 1991. Plagioclase-melt equilibria in hydrous systems. American Mineralogist 76, 477-492.

Kirkpatrick, R.J., Klein, L., Uhlmann, D.R., and Hays, J.F., 1979. Rates and processes of crystal growth in the system anorthite-albite. Journal of Geophysical Research 84, 367l-3676.

Koepke, B., Behrens, H., 2001. Trace element diffusion in andesitic melts: An application of synchrotron X-ray fluorescence analysis. Geochim Cosmochim Acta 65, 1481–1498

Lange, A., Frey, H. M., Hector, J., 2009. A thermodynamic model for the plagioclase-melt hydrometer/thermometer. Am Mineral, 94, 494-506.

L'Heureux, I., 1993. Oscillatory Zoning in Crystal Growth: A Constitutional Undercooling Mechanism. Phys. Rev. E. 48 (6), 4460–4469.

L'Heureux, I., Fowler, A.D., 1996. Dynamical Model of Oscillatory Zoning in Plagioclase with Nonlinear Partition Relation. Geophys. Res. Letters 23 (1), 17–20.

Lasaga, A.C., 1982. Toward a Master Equation in Crystal Growth. Am. J. Sci. 282 (8), 1264–1288.

Liang, Y., Richter, F.M., Watson, E.B., 1996. Diffusion in silicate melts: II. Multicomponent diffusion in CaO-$A1_20_3$-SiO_2 at 1500°C and 1 GPa. Geochimica et Cosmochimica Acta 60 (24), 5021-5035.

Malyshev, A.I., 2000. Life of the volcano. Ural Branch of Russian Academy of Sciences, Ekaterinburg, 262 pp.

Martel, C., Schmidt, B.C., 2003. Decompression experiment insight into ascent rates of silicic magmas. Contrib Mineral Petrol 144, 397-415.

Melnik, O., Sparks, R.S.J., 2005. Controls on Conduit Magma Flow Dynamics during Lava Dome Building Eruptions. J. Geophys. Res. 110 (B2), B02209.

Melnik, O.E., Blundy, J.D., Rust, A.C., Muir, D.D., 2011. Subvolcanic plumbing systems imaged through crystal size distributions. Geology, 39 (4), 403-406.

Melnik, O.E., Sparks, R.S.J., 1999. Non-linear dynamics of lava dome extrusion. Nature 402, 37 – 41.

Mollard, E., Martel, C., Bourdier, J.L., 2012. Decompression-induced crystallization in hydrated silica-rich melts: empirical models of experimental plagioclase nucleation and growth kinetics. J. Petrol 53 (8), 1743-1766.

Moore, G., Vennemann, T., Carmichael, I.S.E., 1998. An empirical model for the solubility of H_2O in magmas to 3 kilobars. American Mineralogist 83, 36–42.

J.E. Mungall, D.B. Dingwell, M. Chaussidon Chemical diffusivities of 18 trace elements in granitoid melts. Geochim. Cosmochim. Acta, 63 (1999), pp. 2599–2610

Murphy, M. D., Sparks, R. S. J., Barclay, J., Carroll, M. R. & Brewer, T. S. (2000). Remobilisation of andesite magma by intrusion of mafic magma at the Soufrière Hills volcano, Montserrat, West Indies. Journal of Petrology 41, 21–42.

Oishi, Y., 1965. Analysis of Ternary Diffusion: Solutions of Diffusion Equations and Calculated Concentration Distribution. J. Chem. Phys. 43 (5), 1611–1620.

Pletchov, P.Yu., Gerya T.V., 1998. Effect of H2O on plagioclase-melt equilibrium. Experiment in GeoSciences 7 (2), 7–9.

Putirka, K.A., 2005. Igneous thermometers and barometers based on plagioclase plus liquid equilibria: Tests of some existing models and new calibrations. Am Mineral 90 (2-3), 336-346.

Rutherford M.J., Devine J.D., 2008, Magmatic conditions and processes in the storage zone of the 2004–2006 Mount St. Helens dacite, in Sherrod D.R., eds., A volcano rekindled; the renewed eruption of Mount St. Helens, 2004–2006: U.S. Geological Survey Professional Paper 1750, p. 703–725.

Shcherbakov, V.D., Plechov, P.Yu., Izbekov, P.E., Shipman J,S., 2011. Plagioclase zoning as an indicator of magma processes at Bezymianny Volcano, Kamchatka. Contributions to Mineralogy and Petrology 162 (1), 83-99.

Tsune, A., Toramaru, A., 2007. A Simple Model of Oscillatory Zoning in Magmatic Plagioclase: Development of an Isothermal Undercooling Model. Am. Mineral. 92 (7), 1071–1079.

Watkins, J.M., DePaolo, D.J., Ryerson, F.J., Peterson, B.T., 2011. Influence of liquid structure on diffusive isotope separation in molten silicates and aqueous solutions. Geochimica et Cosmochimica Acta 75 (11), 3103–3118.

Zhang, Y., Ni, H., Chen, Y., 2010. Diffusion Data in Silicate Melts. Reviews in Mineralogy & Geochemistry 72, 311-408.

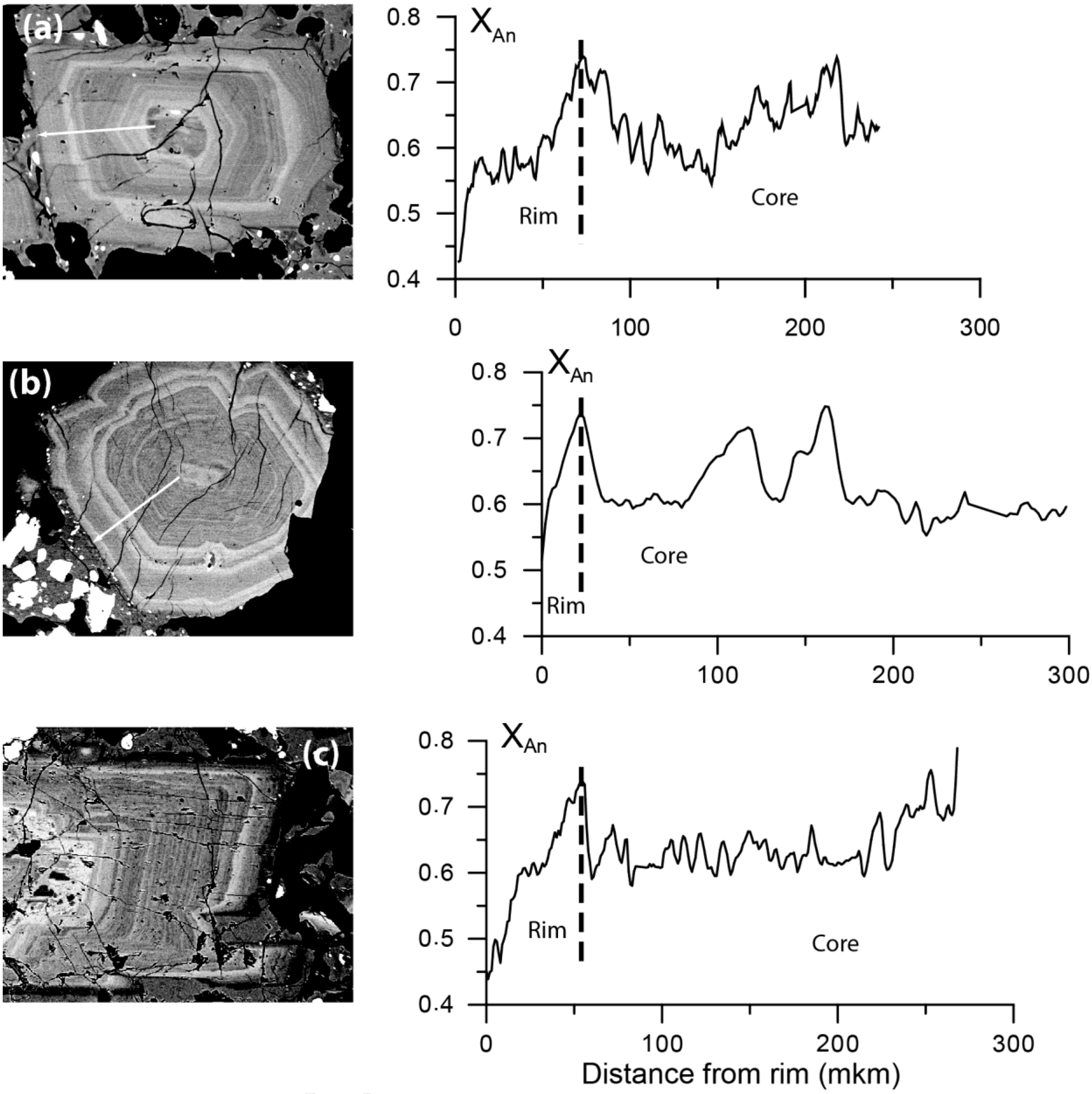
(a)
0.8
0.7
0.6
0.5
0.4
X_{An}
Rim
Core
0
100
200
300
(b)
X_{An}
Rim
Core
(c)
X_{An}
Rim
Core
Distance from rim (mkm)

Figure 1

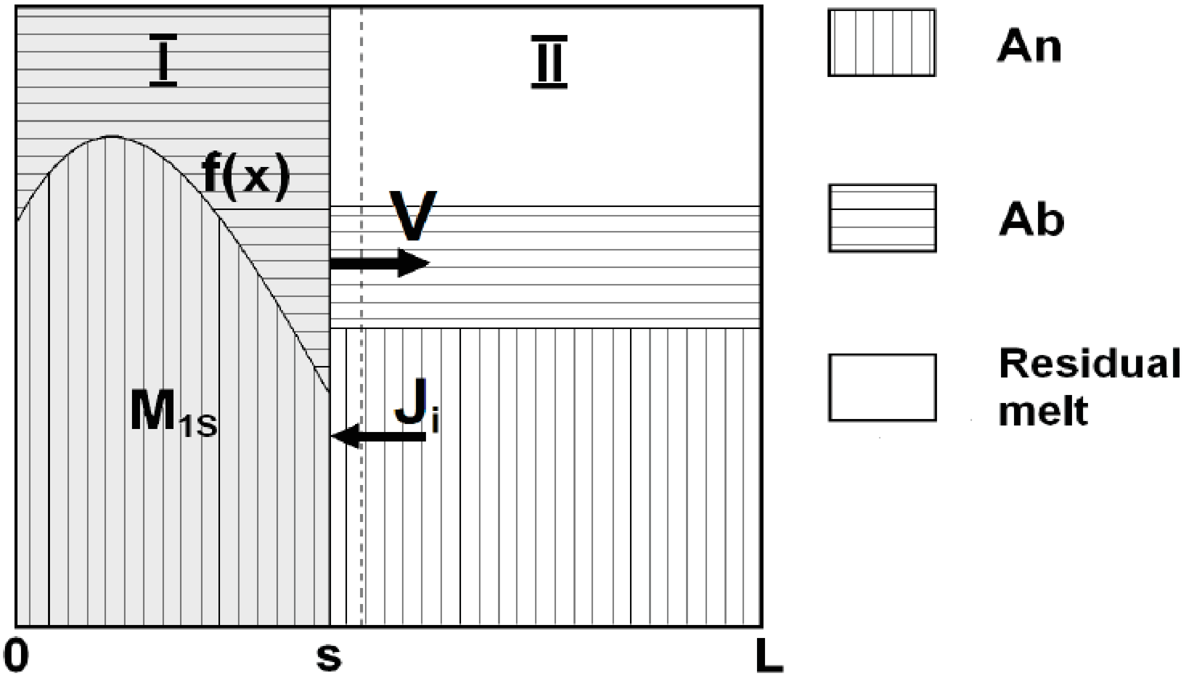

Figure 2

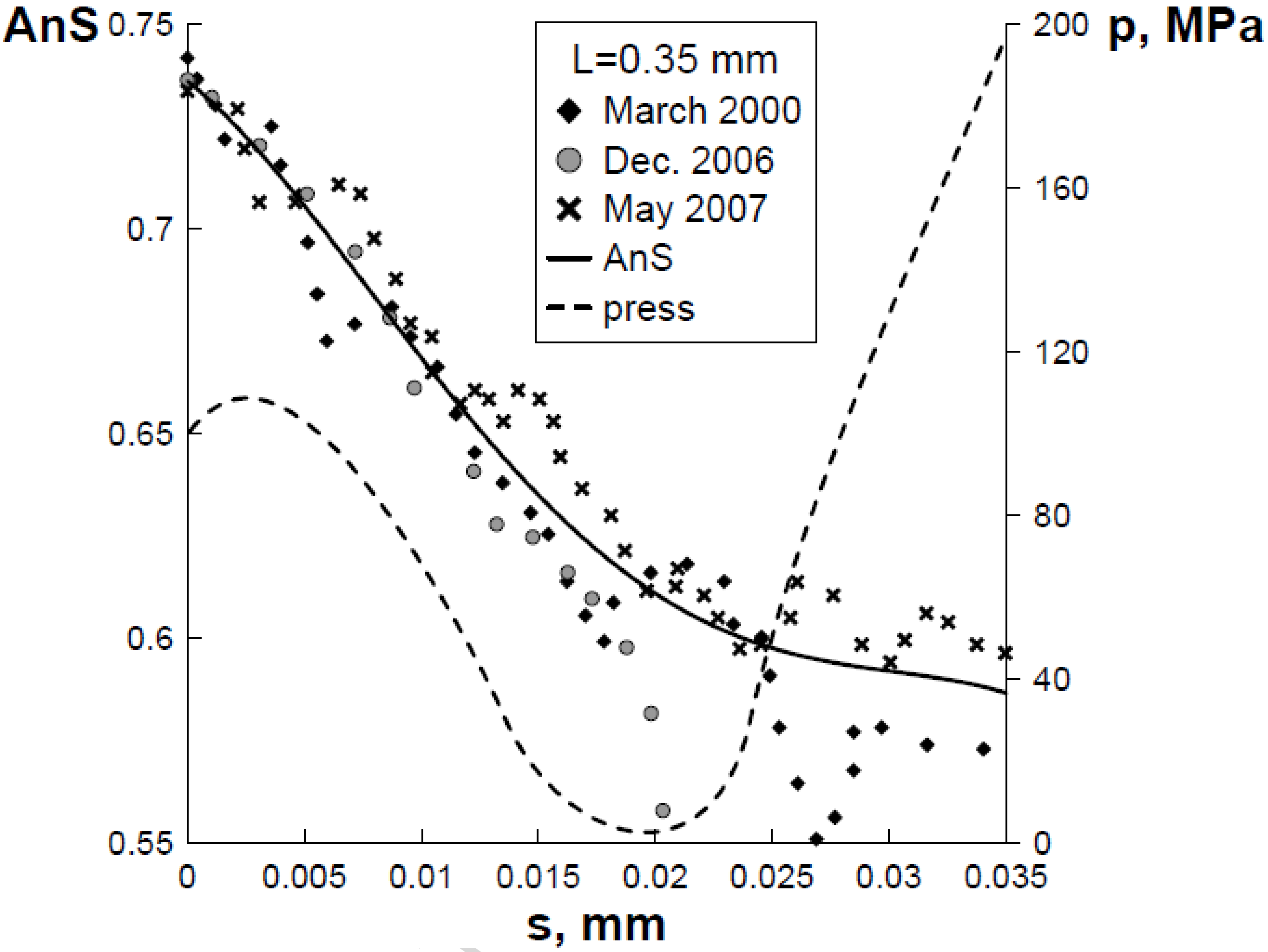
AnS
0.75
0.7
0.65
0.6
0.55
200
160
120
80
40
0
p, MPa
L=0.35 mm
March 2000
Dec. 2006
May 2007
AnS
press
0
0.005
0.01
0.015
0.02
0.025
0.03
0.035
s, mm

Figure 3

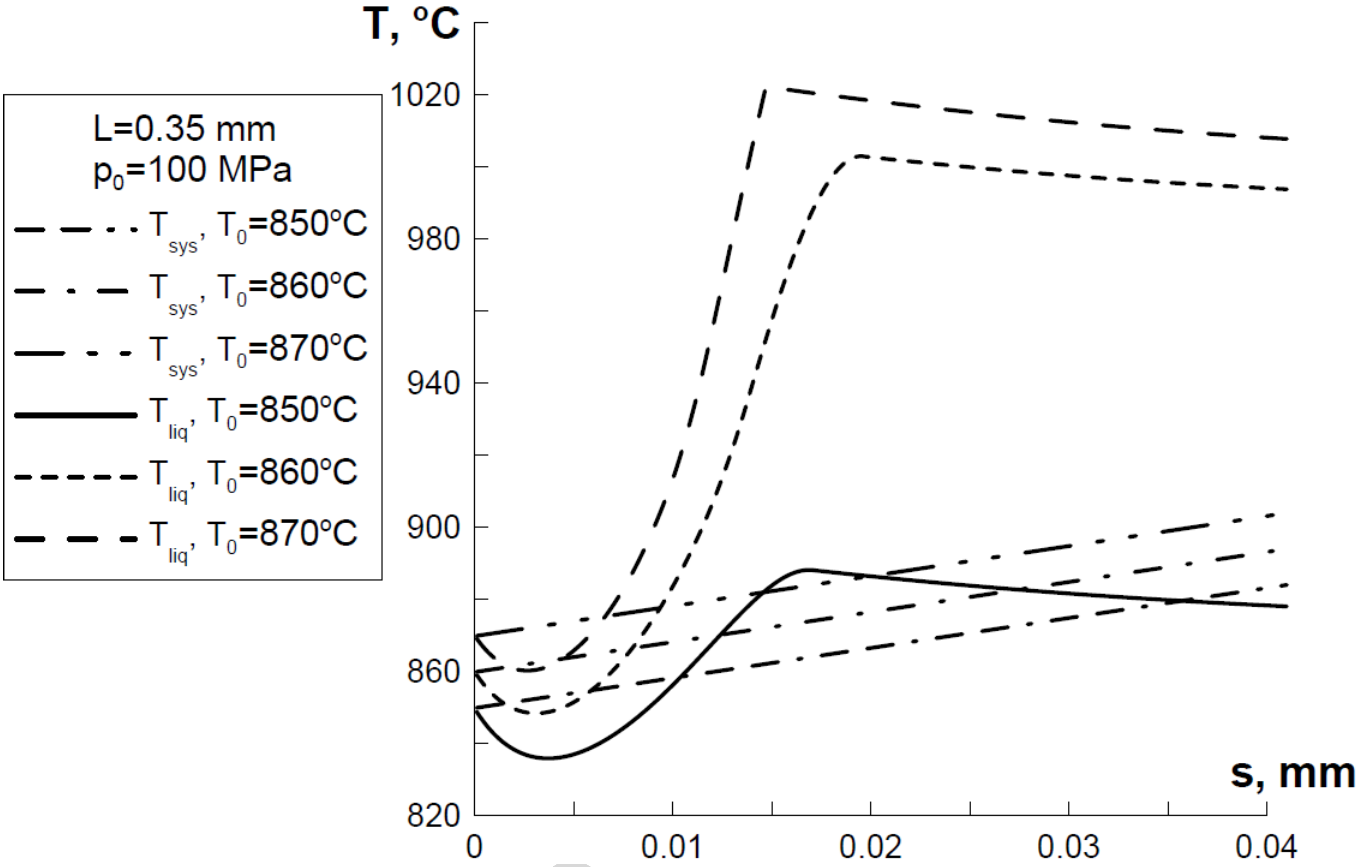
T, °C
1020
980
940
900
860
820
0
0.01
0.02
0.03
0.04
s, mm
L=0.35 mm
p_0=100 MPa
T_{sys}, T_0=850°C
T_{sys}, T_0=860°C
T_{sys}, T_0=870°C
T_{liq}, T_0=850°C
T_{liq}, T_0=860°C
T_{liq}, T_0=870°C

Figure 4A

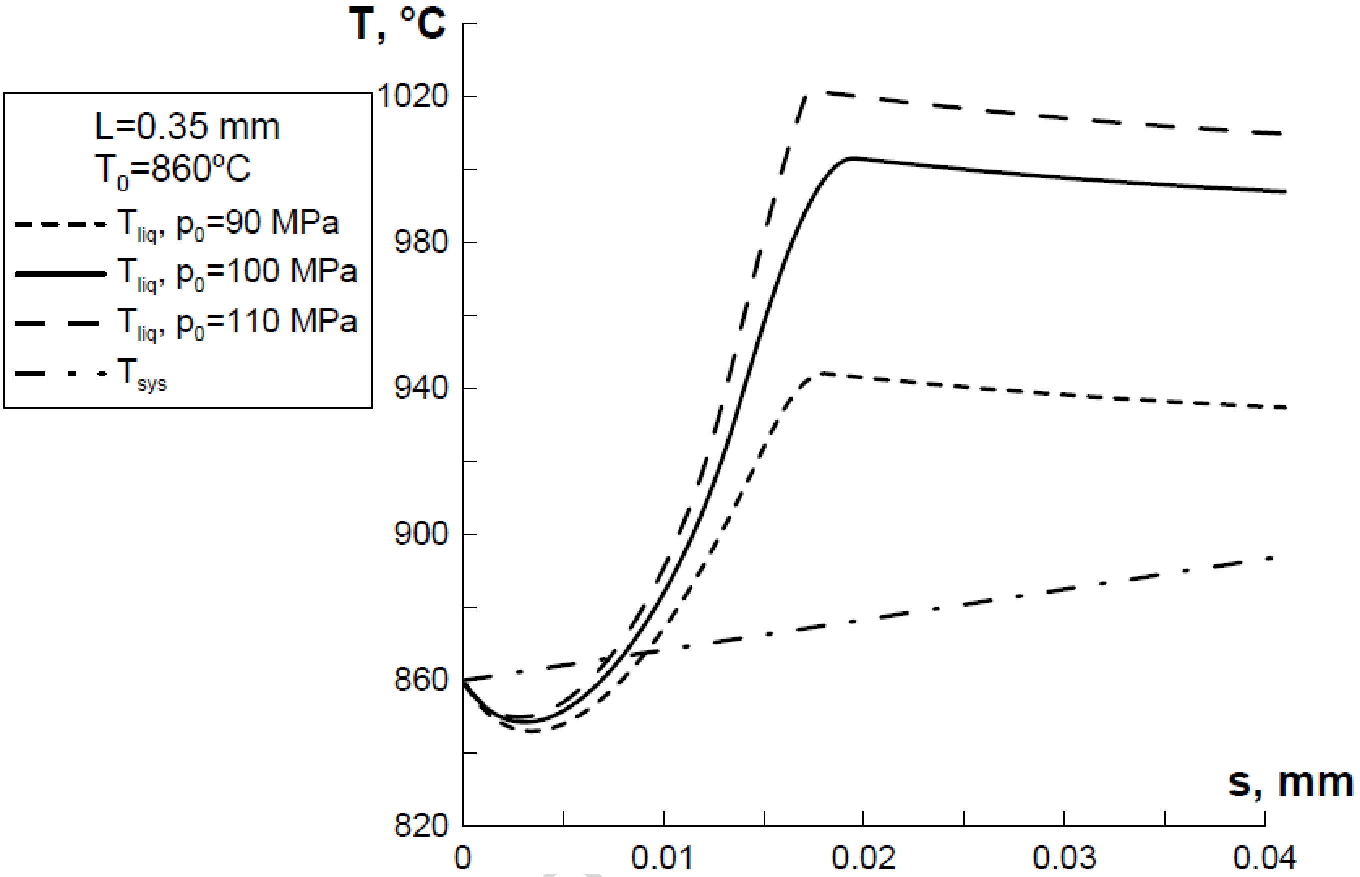
T, °C
1020
980
940
900
860
820
s, mm
0
0.01
0.02
0.03
0.04
L=0.35 mm
T0=860°C
Tliq, p0=90 MPa
Tliq, p0=100 MPa
Tliq, p0=110 MPa
Tsys

Figure 4B

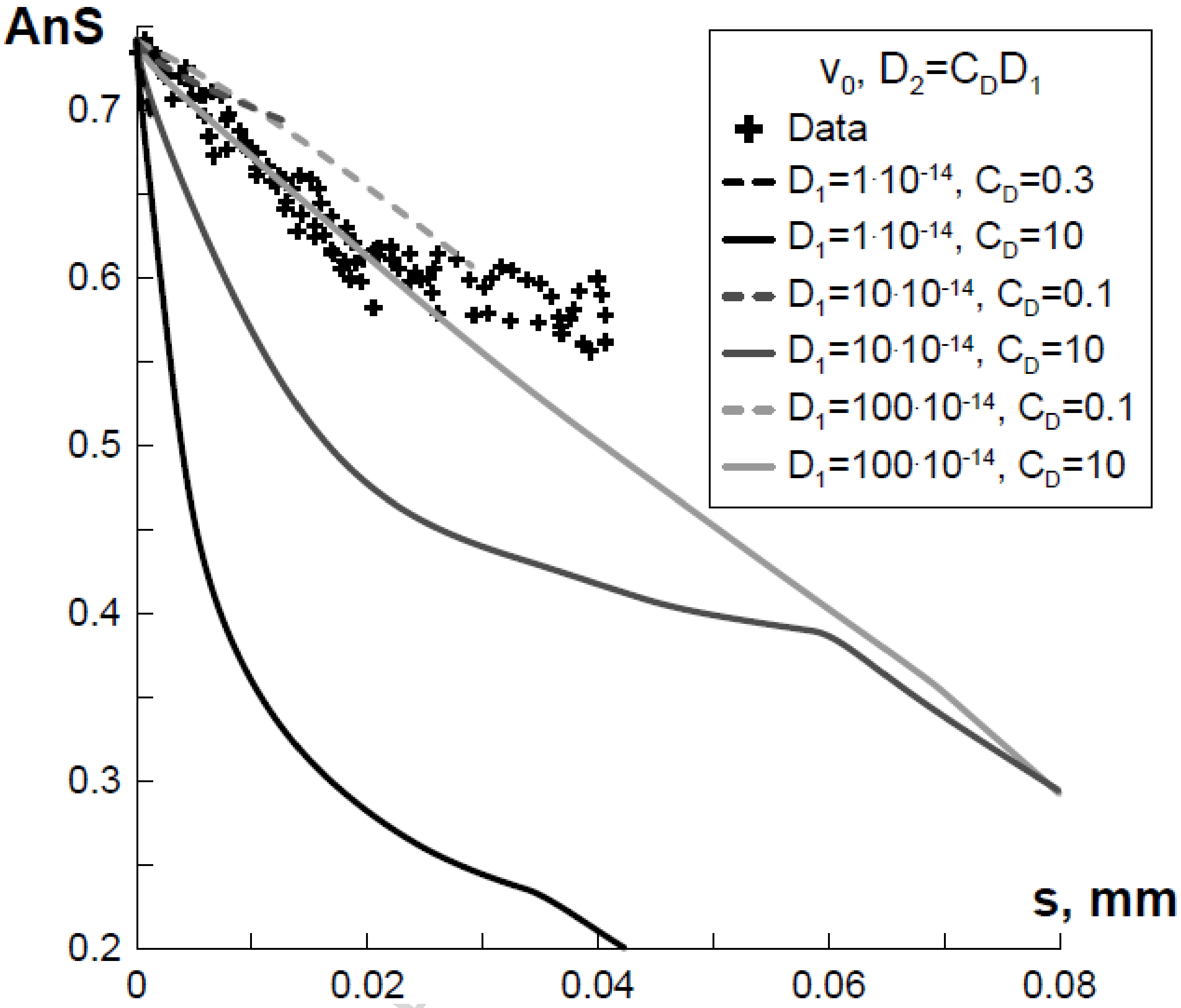
AnS
0.7
0.6
0.5
0.4
0.3
0.2
0
0.02
0.04
0.06
0.08
s, mm
v_0, $D_2=C_DD_1$
Data
$D_1=1\cdot10^{-14}$, $C_D=0.3$
$D_1=1\cdot10^{-14}$, $C_D=10$
$D_1=10\cdot10^{-14}$, $C_D=0.1$
$D_1=10\cdot10^{-14}$, $C_D=10$
$D_1=100\cdot10^{-14}$, $C_D=0.1$
$D_1=100\cdot10^{-14}$, $C_D=10$

Figure 5A

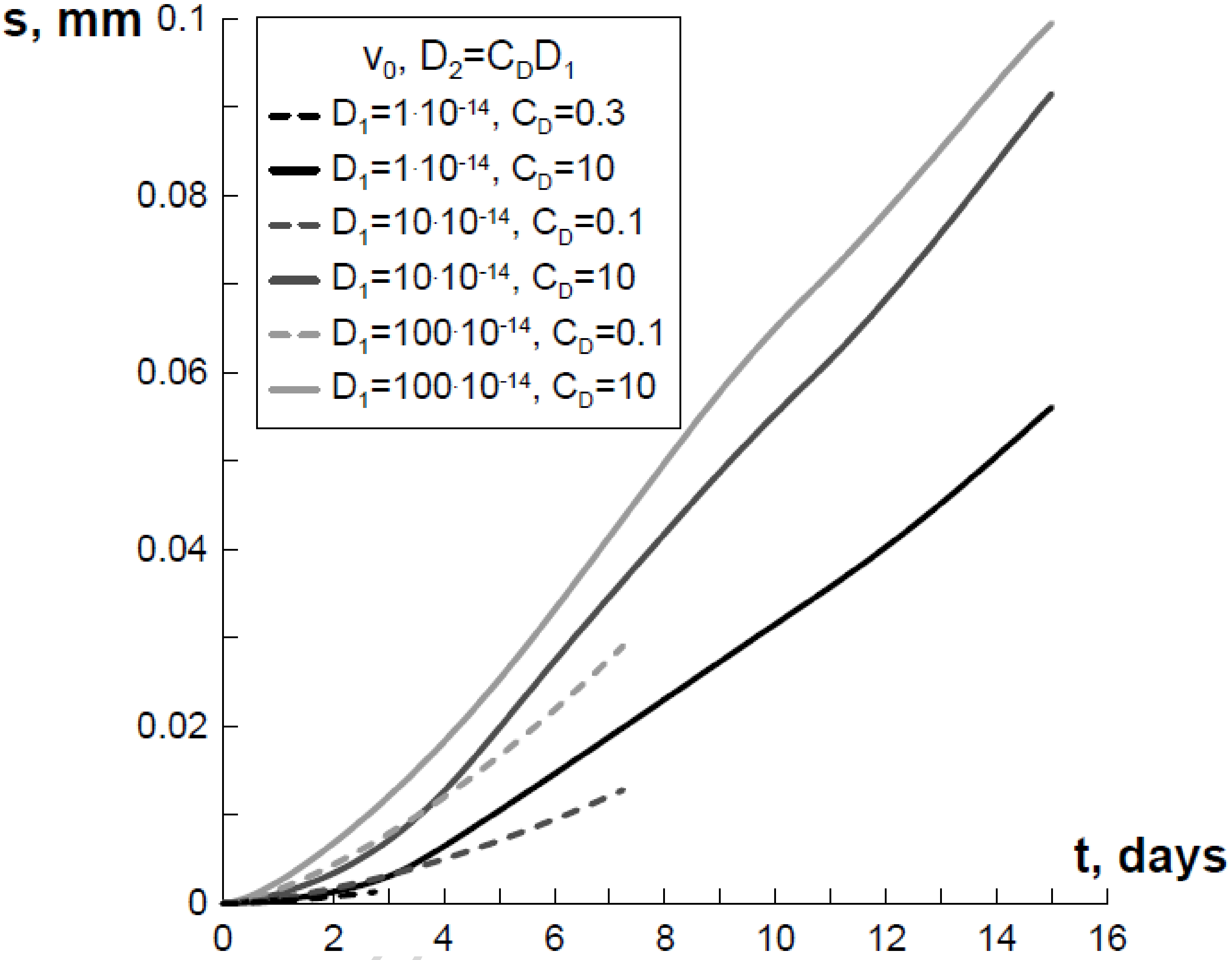
s, mm
0.1
0.08
0.06
0.04
0.02
0
v_0, $D_2=C_DD_1$
$D_1=1\cdot10^{-14}$, $C_D=0.3$
$D_1=1\cdot10^{-14}$, $C_D=10$
$D_1=10\cdot10^{-14}$, $C_D=0.1$
$D_1=10\cdot10^{-14}$, $C_D=10$
$D_1=100\cdot10^{-14}$, $C_D=0.1$
$D_1=100\cdot10^{-14}$, $C_D=10$
t, days
0
2
4
6
8
10
12
14
16

Figure 5B

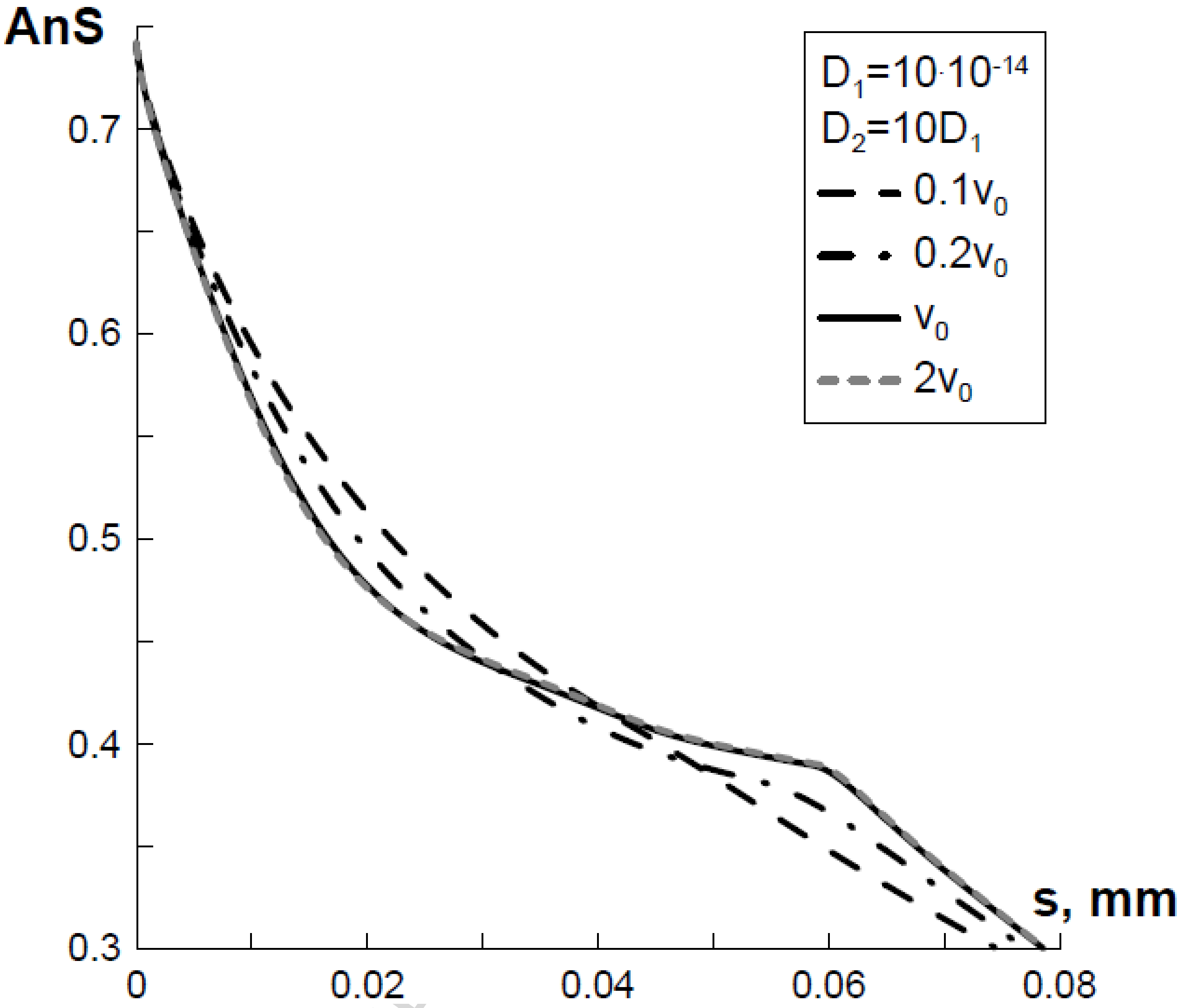
AnS
0.7
0.6
0.5
0.4
0.3
0
0.02
0.04
0.06
0.08
s, mm
$D_1=10\cdot10^{-14}$
$D_2=10D_1$
$0.1v_0$
$0.2v_0$
v_0
$2v_0$

Figure 6A

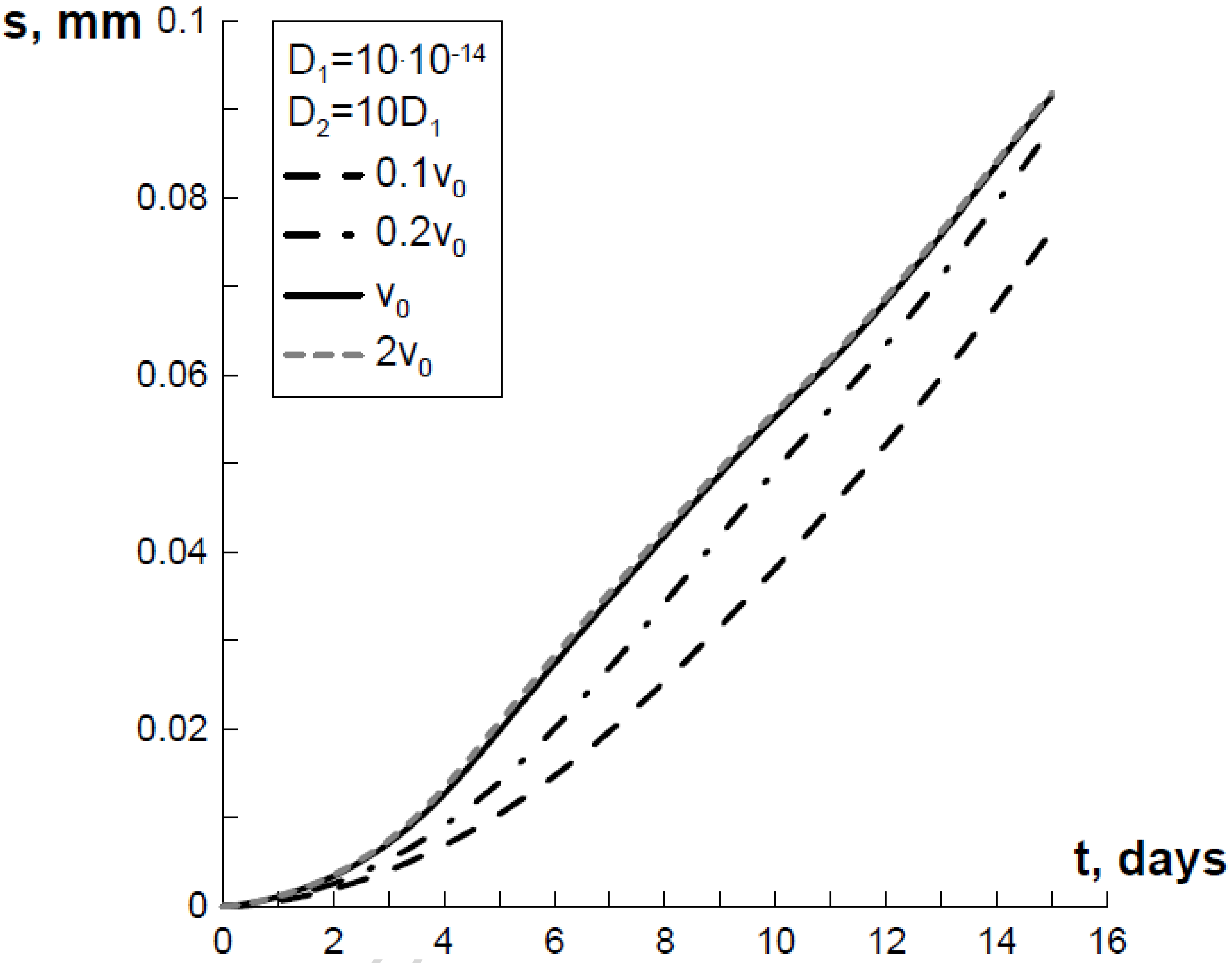
s, mm
t, days
D_1=10·10^{-14}
D_2=10D_1
0.1v_0
0.2v_0
v_0
2v_0
0
0.02
0.04
0.06
0.08
0.1
0
2
4
6
8
10
12
14
16

Figure 6B

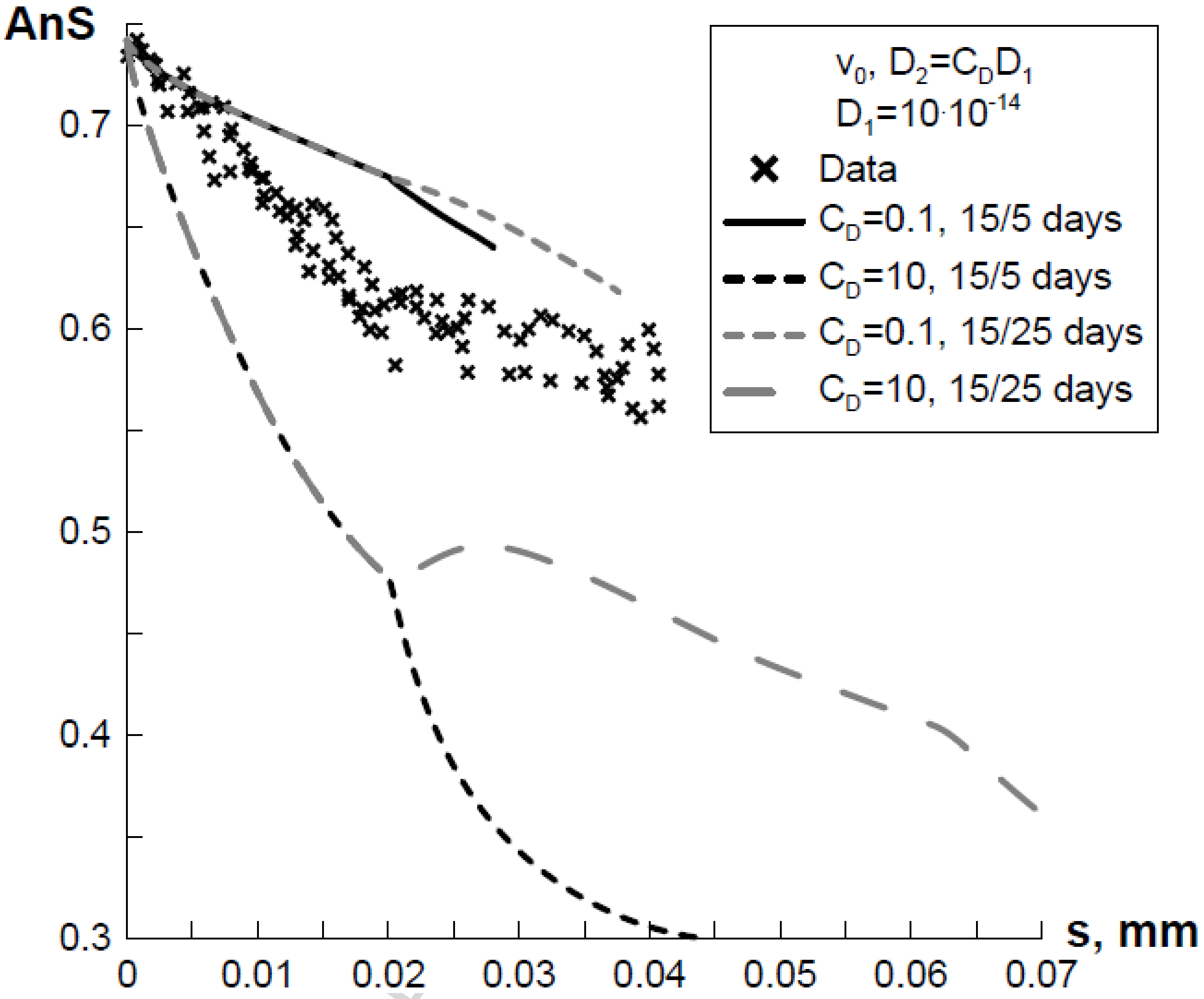
AnS
0.3
0.4
0.5
0.6
0.7
0
0.01
0.02
0.03
0.04
0.05
0.06
0.07
s, mm
v_0, D_2=$C_D D_1$
D_1=10·10^{-14}
Data
C_D=0.1, 15/5 days
C_D=10, 15/5 days
C_D=0.1, 15/25 days
C_D=10, 15/25 days

Figure 7A

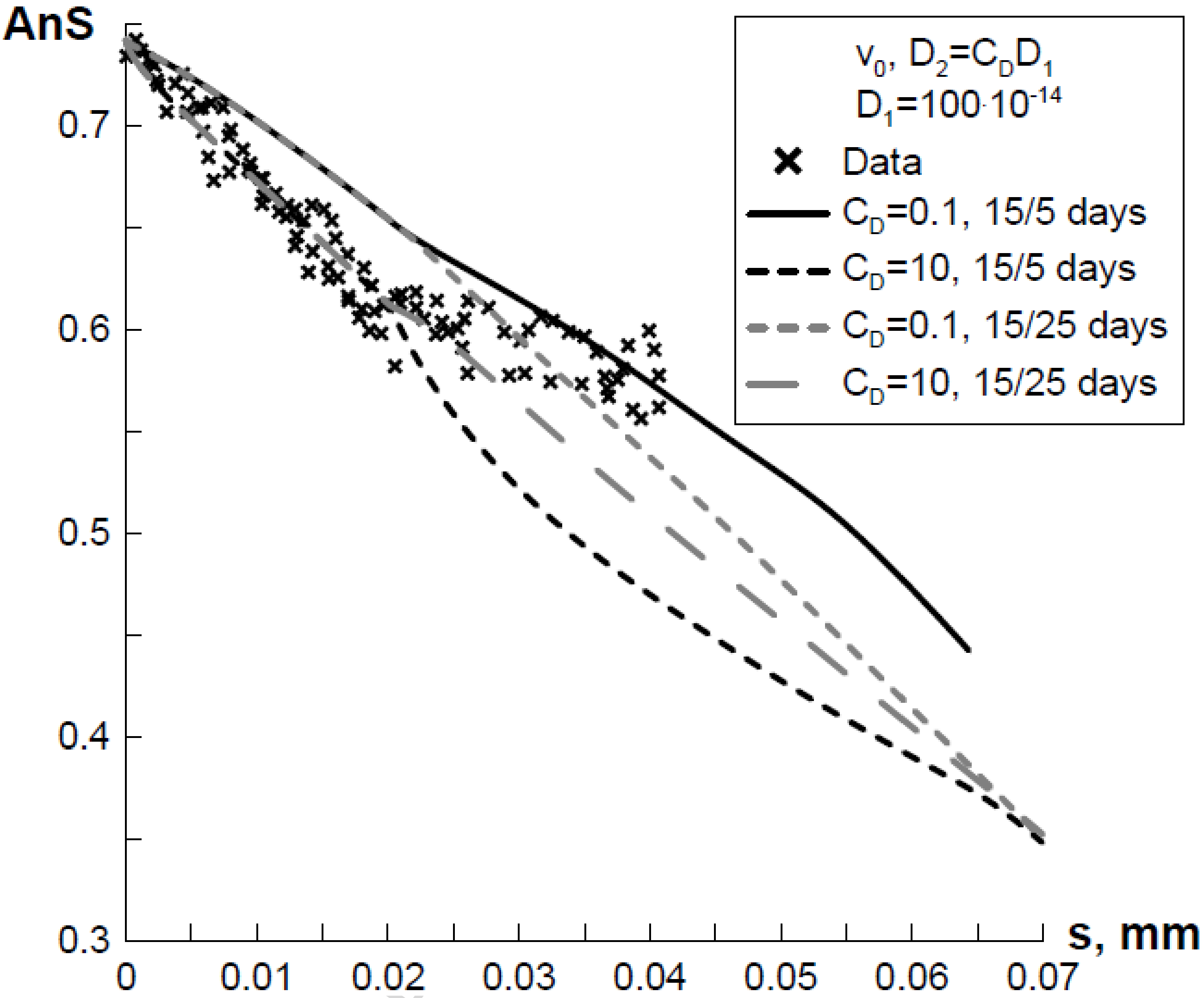
AnS
0.7
0.6
0.5
0.4
0.3
s, mm
0
0.01
0.02
0.03
0.04
0.05
0.06
0.07
v_0, $D_2=C_DD_1$
$D_1=100\cdot10^{-14}$
× Data
C_D=0.1, 15/5 days
C_D=10, 15/5 days
C_D=0.1, 15/25 days
C_D=10, 15/25 days

Figure 7B

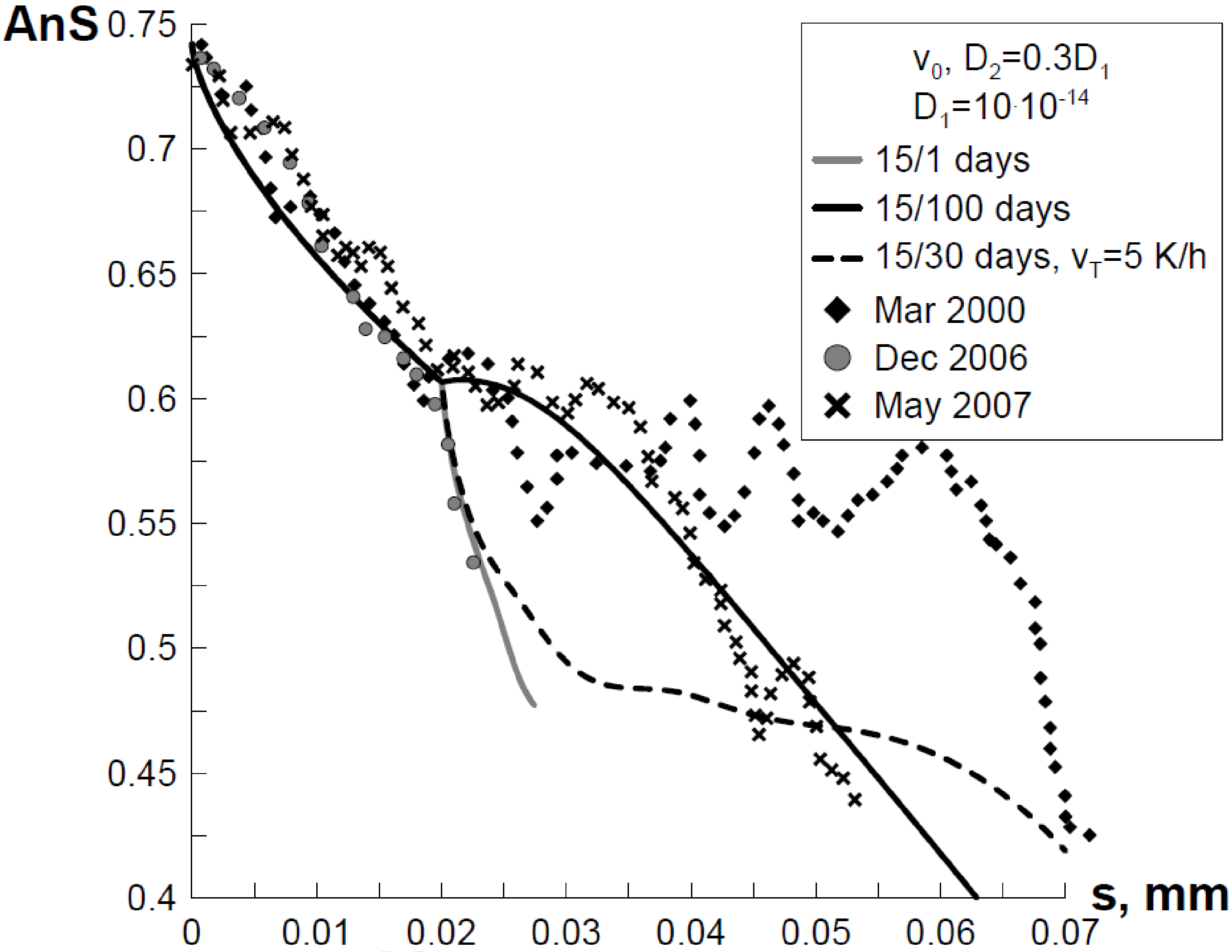
AnS
0.75
0.7
0.65
0.6
0.55
0.5
0.45
0.4
0
0.01
0.02
0.03
0.04
0.05
0.06
0.07
s, mm
v0, D2=0.3D1
D1=10·10-14
15/1 days
15/100 days
15/30 days, vT=5 K/h
Mar 2000
Dec 2006
May 2007

Figure 8

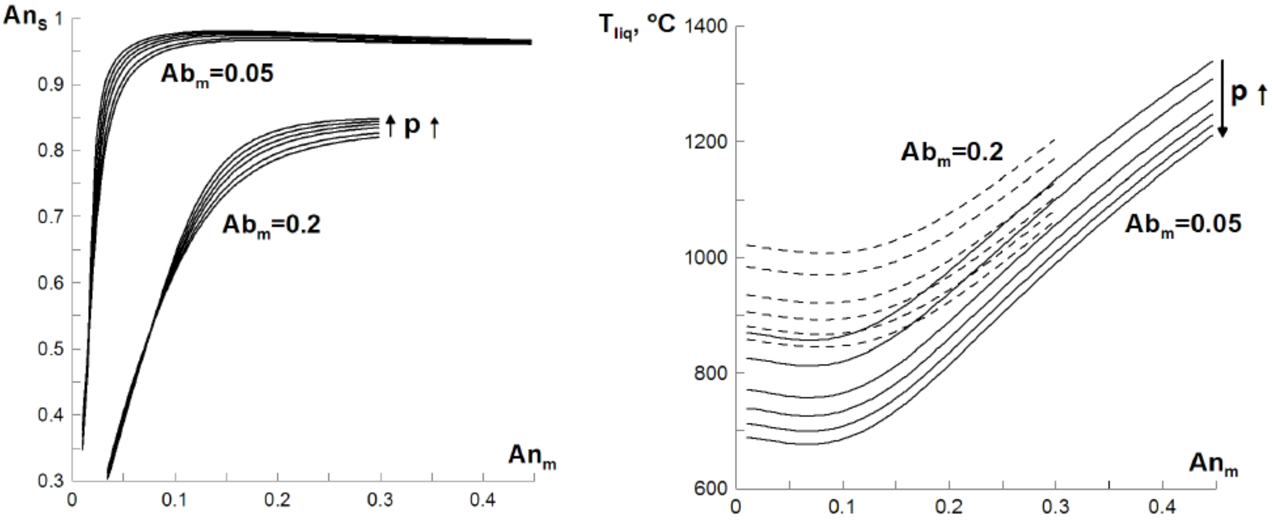
An_s
1
0.9
0.8
0.7
0.6
0.5
0.4
0.3
0
0.1
0.2
0.3
0.4
An_m
Ab_m=0.05
Ab_m=0.2
↑ p ↑
T_{liq}, °C
1400
1200
1000
800
600
0
0.1
0.2
0.3
0.4
An_m
Ab_m=0.2
Ab_m=0.05
p ↑

Figure A1

Highlights

► Slow diffusion in plagioclase preserves information on magma ascent conditions. ► We develop a numerical model of plagioclase rim growth. ► The model is based on multicomponent diffusion equations. ► Results allow estimating magma ascent times for individual crystals.